Understanding the photon-photon resonance of DBR lasers using mode expansion method

Da Chen
Huazhong University of Science and Technology
Ye Liu
Huazhong University of Science and Technology
Yonglin Yu (yonglinyu@mail.hust.edu.cn)
Huazhong University of Science and Technology https://orcid.org/0000-0002-2422-7774

Research Article

Keywords: Direct modulated lasers, Photon-photon resonance, Mode expansion, Mode interaction

Posted Date: November 29th, 2021

DOI: https://doi.org/10.21203/rs.3.rs-1027265/v1

Understanding the photon-photon resonance of DBR lasers using mode expansion method

Da Chen, Ye Liu, Yonglin Yu*
Wuhan National Laboratory for Optoelectronics, Huazhong University of Science and Technology, Wuhan 430074, P. R. China
(*author for correspondence: Email: yonglinyu@mail.hust.edu.cn)

Abstract
A theoretical model based on the mode expansion of the traveling wave equations is developed to investigate the mode interaction processes behind the photon-photon resonance (PPR) effect in distributed Bragg reflector (DBR) lasers. With dual-mode rate equations, strength of mode interactions is characterized by the cross power and the coupling factors, which arise from the non-orthogonality of the main mode and the PPR mode. Small signal analysis and large-signal dynamics are performed, and results indicate that the cross power is a key contributor to the PPR effect.

Keywords Direct modulated lasers, Photon-photon resonance, Mode expansion, Mode interaction

1 Introduction

Direct modulated lasers (DMLs) have advantages of high energy efficiency and small size, which are attractive for data centers, metro access networks and other short-distance optical communication systems. The bandwidth of DMLs can be significantly increased by three intracavity effects: detuned-loading effect, high-pass filter effect, and photon-photon resonance (PPR) effect (Matsui 2017). The detuned-loading effect increases the effective differential gain and relaxation oscillation frequency by using the negative feedback of the Bragg grating (Kjebon and Schatz 1997). The high-pass filter effect reduces the roll-off rate of the modulation response at high frequencies (Matsui 2017), which is similar to the Q-modulation of the laser (He 2007). The PPR effect extends the modulation bandwidth with a help of a side mode, introducing an additional resonance peak in the modulation response curve (Morthier 2000). Furthermore, properly combining these three effects can significantly improve the bandwidth of DMLs (Mieda 2016, Matsui 2021).

Compared to the detuned-loading effect and the high-pass filter effect, which are only related to the main mode, the PPR effect originates from the multimode dynamics of semiconductor lasers. The PPR effect is first predicted to appear in lasers with short-cavity optical feedback and is interpreted as resonance enhancement near the multimode stability boundary of the Lang-Kobayashi (LK) rate equations (Tager 1993). Although the LK equations can describe the multimode dynamics, the calculated results are qualitative because the cavity structure is neglected. Subsequently, the time-domain traveling wave model (TWM) is used to simulate the PPR effect in multi-section lasers, which considers both the multimode dynamics and the longitudinal structure of the cavity (Morthier 2000, Bardella 2013). However, the results of the TWM cannot reveal interactions between

different modes of the lasers, especially for special designed multi-section lasers. For this reason, the mode expansion method of the traveling wave equations was developed to explain the PPR effect in passive-feedback lasers (Radziunas 2007), which includes a set of ordinary differential equations for the complex amplitudes of the different modes, and where the coupling factors feature the driving force of the multimode dynamics (Radziunas 2005).

In this paper, we extend the mode expansion method to investigate mode dynamics of DBR lasers when the PPR occurs. A cross-power term is naturally obtained by expanding the total optical power into different modes, which also drives the multimode dynamics. To understand improvements in modulation efficiency due to the PPR effect, variations of the cross power and the coupling factors with wavelength detuning are simulated and discussed. Finally, small-signal analysis and large signal dynamics are performed. Results reveal the main components of the PPR peak and demonstrate how the cross power initiates the PPR effect.

2 Modal expansion of the traveling wave equations

The cavity of a laser is always open and dissipative. Photons are generated by stimulated emission, lasing out of the mirror, and finally form a stable longitudinal spatial distribution in the cavity. However, this stable field distribution is not a "true mode" but a "quasi mode", which means that different longitudinal modes are not completely power orthogonal, and can be coupled with each other.

For a semiconductor laser, the slowly varying amplitudes of the forward and backward traveling waves can be denoted as $E^{+}(z,t)$ and $E^{-}(z,t)$. Assuming that there is a main mode and a side mode (PPR mode) in the DBR laser, the envelops of the electric field can be decomposed into:

$$\begin{bmatrix} E^{+}(z,t) \\ E^{-}(z,t) \end{bmatrix} = f_1(t)\begin{bmatrix} \Phi_1^{+}(z) \\ \Phi_1^{-}(z) \end{bmatrix} + f_2(t)\begin{bmatrix} \Phi_2^{+}(z) \\ \Phi_2^{-}(z) \end{bmatrix} \tag{1}$$

where the subscripts 1 and 2 indicate the main mode and PPR mode, respectively. The coefficients $f_{1,2}(t)$ represent the time-dependent complex amplitudes of the main mode and PPR mode, while the forward and backward electric field patterns $\Phi_{1,2}^{+,-}(z)$ of these two modes are calculated at the threshold and are considered constant above the threshold. The electric field patterns of a multi-section laser are defined as eigenfunctions of the traveling wave equations, which can be solved by the transfer matrix method (Radziunas 2005).

According to the definition of the electromagnetic field energy density (Feiste 1998) and the mode expansion equation (1), the photon density in the active section can be expressed as the extended form:

$$\begin{aligned} S_{\mathrm{a}}(t) &= \int_0^{L_{\mathrm{a}}} \left[\left|E^{+}(z,t)\right|^2 + \left|E^{-}(z,t)\right|^2 \right] \mathrm{d}z \\ &= \left|f_1(t)\right|^2 \int_0^{L_{\mathrm{a}}} \left[\left|\Phi_1^{+}(z)\right|^2 + \left|\Phi_1^{-}(z)\right|^2 \right] \mathrm{d}z \\ &+ \left|f_2(t)\right|^2 \int_0^{L_{\mathrm{a}}} \left[\left|\Phi_2^{+}(z)\right|^2 + \left|\Phi_2^{-}(z)\right|^2 \right] \mathrm{d}z \\ &+ 2\,\mathrm{Re}\left\{ f_1(t) f_2^{*}(t) \int_0^{L_{\mathrm{a}}} \left[\Phi_1^{+}(z)\Phi_2^{+*}(z) + \Phi_1^{-}(z)\Phi_2^{-*}(z) \right] \mathrm{d}z \right\} \end{aligned} \tag{2}$$

where the integral is only calculated within the active section $[0, L_{\mathrm{a}}]$. Clearly, on the right-hand side, the first two terms represent the photon densities of the main mode S_1 and the PPR mode S_2, respectively. It is noteworthy that the third term, which can be understood as a "cross power S_{X}" between the main mode and PPR mode, is due to the power non-orthogonality of longitudinal modes of the open cavity. Accordingly, we have $S_{\mathrm{a}} = S_1 + S_2 + S_{\mathrm{X}}$. Similar to that seen in the coupled waveguides, the cross-power term is thought to be related to the energy exchange between modes in different waveguides, which can be used

to explain the crosstalk in directional couplers (Huang 1994). Here, the cross power between different longitudinal modes is found to be the main contributor to the PPR effect, and simulation results in Section 4 will demonstrate this.

Considering dual-mode expansion of the traveling wave equations, following dual-mode rate equations can be derived (Feiste 1998):

$$\frac{df_1}{dt} = \left(i\Omega_1 + K_{11}\right) f_1(t) + K_{12} f_2(t) \tag{3}$$

$$\frac{df_2}{dt} = \left(i\Omega_2 + K_{22}\right) f_2(t) + K_{21} f_1(t) \tag{4}$$

$$\frac{dN_a}{dt} = \frac{I_a(t)}{eV_a} - \frac{N_a(t)}{\tau_N} - \upsilon_g g_N \frac{N_a(t) - N_{tr}}{1 + \varepsilon S_a(t)} S_a(t) \tag{5}$$

where the amplitude equations (3) and (4) are coupled with the carrier equation (5) through the photon density (2). The eigenvalues $\Omega_{1,2}$ can be solved by the transfer matrix method mentioned above. The coupling factors K_{nm} (n, m = 1, 2) of the DBR laser are defined as (Feiste 1998):

$$K_{nm} = -i\upsilon_g \Delta\beta_a \int_0^{L_a} \left[\Phi_n^+(z)\Phi_m^-(z) + \Phi_n^-(z)\Phi_m^+(z)\right] dz \tag{6}$$

$$\Delta\beta_a = i\frac{1}{2}(1 + i\alpha_H)\Gamma_{xy} g_N \left(N_a - N_{th}\right) \tag{7}$$

where the carrier density N_a and wavevector detuning $\Delta\beta_a$ are considered to be spatially constant within the active section. However, for multi-section lasers, variations of wavevector in one section will change the wavevector profile of the whole device, which leads to coupling between different modes and non-zero cross-coupling factors K_{12} and K_{21} (Radziunas 2005).

3 Small-Signal Modulation Response

A sinusoidal modulated signal is loaded to the bias current with a modulation frequency ω and a small amplitude δI_a. Subsequently, the complex amplitudes of the main mode f_1 and PPR mode f_2, as well as the carrier density N_a will respond at frequency ω around their steady-state values. Replacing the variables in (3)-(4) with their own first-order Taylor expansions and neglecting the higher order terms, we can get the linearized rate equations:

$$\begin{bmatrix} i\omega - i\Omega_1 & 0 & 0 & 0 & -\bar{k}_{11} f_{1s} \\ 0 & i\omega + i\Omega_1^* & 0 & 0 & -\bar{k}_{11}^* f_{1s}^* \\ 0 & 0 & i\omega - i\Omega_2 & 0 & -\bar{k}_{21} f_{1s} \\ 0 & 0 & 0 & i\omega + i\Omega_2^* & -\bar{k}_{21}^* f_{1s}^* \\ \bar{s}_{11} f_{1s}^* & \bar{s}_{11}^* f_{1s} & \bar{s}_{12} f_{1s}^* & \bar{s}_{12}^* f_{1s} & i\omega + \upsilon_g g_N S_{as} + 1/\tau_N \end{bmatrix} \begin{bmatrix} \delta f_1 \\ \delta f_1^* \\ \delta f_2 \\ \delta f_2^* \\ \delta N_a \end{bmatrix} = \begin{bmatrix} 0 \\ 0 \\ 0 \\ 0 \\ \dfrac{\delta I_a}{q V_a} \end{bmatrix} \tag{8}$$

where the superscript * denotes the complex conjugate value and the subscript s denotes the steady-state value. The diagonal terms have two eigenvalues of the main mode (Ω_1, Ω_1^*) and two eigenvalues of the PPR mode (Ω_2, Ω_2^*), which implies that the PPR peak are sharper than the relaxation oscillation peaks, as will be demonstrated in Section 4. The zero elements in the non-diagonal terms are due to the fact that the gain saturation effect has been ignored in the small signal analysis.

The non-zero elements in the non-diagonal terms are related to the overlap integrals in (2) and (6), which are defined as (n, m = 1, 2):

$$s_{nm} = \int_0^{L_a} \left(\Phi_n^{+*}\Phi_m^+ + \Phi_n^{-*}\Phi_m^-\right) dz, \quad \bar{s}_{nm} = \upsilon_g g_N \left(N_{th} - N_{tr}\right) \cdot s_{nm} \tag{9}$$

$$k_{nm} = \int_0^{L_a} \left(\Phi_n^- \Phi_m^+ + \Phi_n^+ \Phi_m^- \right) dz \,, \quad \bar{k}_{nm} = \frac{1}{2} \Gamma_{xy} \upsilon_g g_N \left(1 + i\alpha_H \right) \cdot k_{nm} \tag{10}$$

Using these notations, the photon number and the coupling factors can be written as:

$$S_a = s_{11} \left| f_1(t) \right|^2 + s_{22} \left| f_2(t) \right|^2 + 2\mathrm{Re}\left[s_{12} f_1^*(t) f_2(t) \right] \tag{11}$$

$$K_{nm} = \bar{k}_{nm} \Delta N_a \tag{12}$$

According to (11), the small-signal AM response $\delta S_a/\delta I_a$ of the DBR laser when PPR occurs can be decomposed into three components:

$$\frac{\delta S_1}{\delta I_a} = s_{11} f_{1s}^* \frac{\delta f_1}{\delta I_a} + s_{11}^* f_{1s} \frac{\delta f_1^*}{\delta I_a} \tag{13}$$

$$\frac{\delta S_2}{\delta I_a} = s_{22} f_{2s}^* \frac{\delta f_2}{\delta I_a} + s_{22}^* f_{2s} \frac{\delta f_2^*}{\delta I_a} \tag{14}$$

$$\frac{\delta S_X}{\delta I_a} \approx s_{12} f_{1s}^* \frac{\delta f_2}{\delta I_a} + s_{12}^* f_{1s} \frac{\delta f_2^*}{\delta I_a} \tag{15}$$

where we have $\delta S_a = \delta S_1 + \delta S_2 + \delta S_X$. Considering that f_{2s} is much smaller than f_{1s}, the term with f_{2s} is ignored in (15). The modulation transfer functions (MTFs) $\delta f_1/\delta I_a$, $\delta f_2/\delta I_a$ and their complex conjugates can be calculated by applying the Cramer's rule (Coldren 2012) to the linearized rate equations (8).

4 Simulation results and discussion

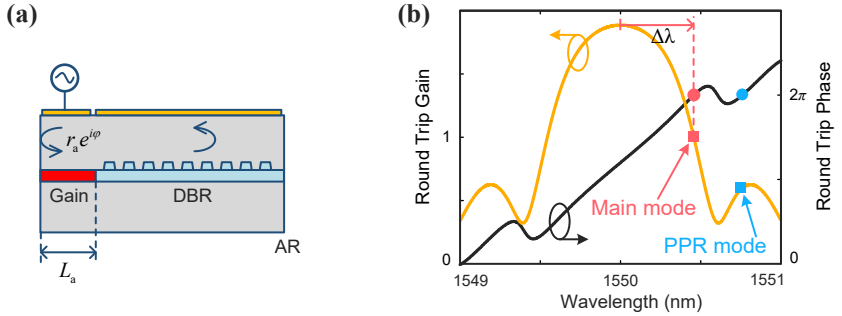

Fig. 1a Schematic of the DBR laser in simulation. **b** Simulated round-trip gain and phase curves of the DBR laser when PPR occurs. Δλ is the detuning of the lasing wavelength with respect to the Bragg wavelength.

To reveal the mode dynamics behind the PPR effect, a two-section DBR laser is used here for simulation, as shown in Fig. 1a. For simplicity, we assume that the lasing wavelength of the DBR laser can be tuned by changing the facet phase ϕ of the active section. The parameters used in our model are listed in Table 1, similar with ones in (Bardella 2013), where the lengths of the gain section and DBR section are set to 100 μm and 660 μm, respectively, corresponding to a PPR frequency of ~45 GHz. The simulated round-trip gain and phase curves of the DBR laser when PPR occurs are plotted in Fig. 1b. It can be seen that the main mode is located on the long wavelength side of the Bragg wavelength with a wavelength detuning of Δλ. The PPR mode is located on the side lobe next to the main lobe, and the frequency interval between the PPR mode and the main mode is equal to the frequency of the PPR peak (PPR frequency).

Table 1 Structure and material parameters of DBR lasers

Description	Symbol	Value	Unit
Length of active section	L_a	100	μm
Volume of active section	V_a	4.8	μm^3
Length of DBR section	L_g	660	μm
Grating coupling coefficient	κ	2000	m^{-1}
Optical confinement factor	Γ_{xy}	0.3	
Effective refractive index	n_{eff}	3.4	
Group velocity	v_g	$3/3.7\times10^8$	
Differential gain	g_N	3×10^{-20}	m^{-3}
Transparency carrier density	N_{tr}	1.5×10^{24}	m^{-3}
Gain compression factor	ε	2×10^{-23}	m^3
Internal absorption	α_0	1000	m^{-1}
Linewidth enhancement factor	α_H	3	
Carrier lifetime	τ_N	1×10^{-9}	s

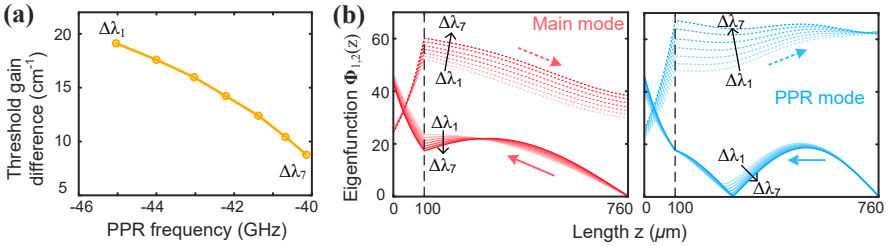

Fig. 2a Eigenvalue of the PPR mode Ω_2 versus $\Delta\lambda$, PPR frequency=$\mathrm{Re}(\Omega_2)/2\pi$, Threshold gain difference= $2\mathrm{Im}(\Omega_2)/v_g$. **b** Amplitudes of the eigenfunctions of the main mode $\mathbf{\Phi}_1(z)$ and PPR mode $\mathbf{\Phi}_2(z)$. Wavelength detuning $\Delta\lambda_{1\text{-}7}$ = 0.371 nm, 0.388 nm, 0.404 nm, 0.419 nm, 0.433 nm, 0.446 nm, 0.457 nm, respectively.

The eigenvalue of the PPR mode Ω_2 versus $\Delta\lambda$ is shown in Fig. 2a, where 7 groups of facet phases ϕ and wavelength detuning $\Delta\lambda$ are selected such that the PPR effect can occur. The frequency detuning of the PPR mode relative to the main mode is $\mathrm{Re}(\Omega_2)/2\pi$, which corresponds to the PPR frequency of 40 to 45 GHz. The threshold gain difference of the PPR mode with respect to the main mode is $2\mathrm{Im}(\Omega_2)/v_g$, which decreases with increasing $\Delta\lambda$, indicating a decrease in side mode suppression ratio (SMSR). The amplitudes of the eigenfunctions of the main mode and the PPR mode are shown in Fig. 2b. As $\Delta\lambda$ increases, the main mode is less concentrated in the active section, while the PPR mode is more concentrated in the active section. The strength of the mode interactions and the PPR are determined by these eigenfunctions, and the quantitative description requires the calculation of their overlap integrals.

The overlap integrals s_{nm} and k_{nm} defined in photon density (9) and coupling factors (10) are calculated, which are then plotted in Fig. 3a and b, respectively. In the DBR laser, when $n = m$, s_{nn} is equal to the product of the longitudinal confinement factor and the square root of the Petermann factor of the nth mode, while k_{nn} is called the reactive confinement factor of the nth mode (Chacinski and Schatz 2010). These two confinement factors describe the concentration of the mode in the active section. The red triangle represents the confinement factors of the main mode, whose amplitude decreases with increasing $\Delta\lambda$, while the blue square represents those of the PPR mode, whose amplitude increases with increasing $\Delta\lambda$. The variations of the confinement factors are consistent with the findings in Fig. 2b.

The green circles in Fig. 3a and b represent s_{nm} and k_{nm} ($n \neq m$), which are related to the cross power and cross-coupling factors, respectively. When $\Delta\lambda$ increases, the amplitudes of these cross terms increase, which means that the non-orthogonality between the main mode and the PPR mode increases, and thus the strength of the mode interactions are enhanced.

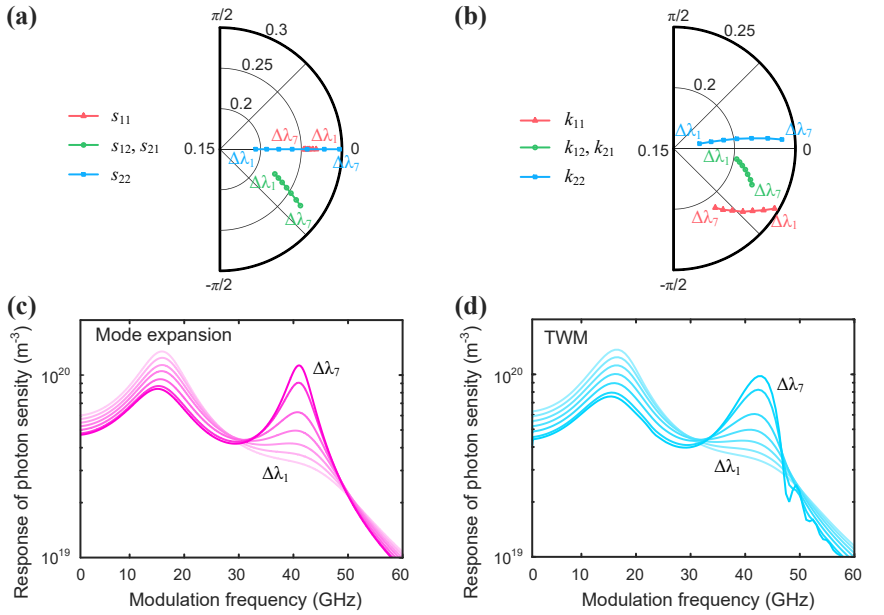

Fig. 3a and **b** Overlap integrals s_{nm} and k_{nm} versus Δλ. **c** and **d** Small-signal responses calculated by the mode expansion rate equations and TWM. $\Delta\lambda_{1\text{-}7}$ = 0.371 nm, 0.388 nm, 0.404 nm, 0.419 nm, 0.433 nm, 0.446 nm, 0.457 nm, respectively.

Thereafter, the small-signal responses of the DBR laser calculated by the mode expansion rate equations (3)-(5) and TWM are compared in Fig. 3c and d, where the bias current of the active section is set at 20 mA. Clearly, results of the mode expansion method and TWM are in good agreement. The relaxation oscillation peak is located at ~16 GHz, while the PPR peak is located at ~41 GHz. Furthermore, the strength of the PPR effect increases with increasing Δλ, which can be interpreted as a result of a decrease in the threshold gain difference $2\text{Im}(\Omega_2)/v_g$ and an increase in the cross terms s_{nm} and k_{nm} $(n \neq m)$. Small signal analysis is needed to determine the relationship between these factors and the PPR response.

As shown in (11), the optical power in the active section can be decomposed into three components: main mode power S_1, PPR mode power S_2, and cross power S_X. The small signal responses of these three components are calculated by (13)-(15) and then plotted in Fig. 4, where Δλ = 0.446 nm. The small signal response of the total optical power $\delta S_a/\delta I_a$ (black line) exhibits a PPR peak at 41 GHz, so the 3dB bandwidth of the DBR laser can reach 50 GHz.

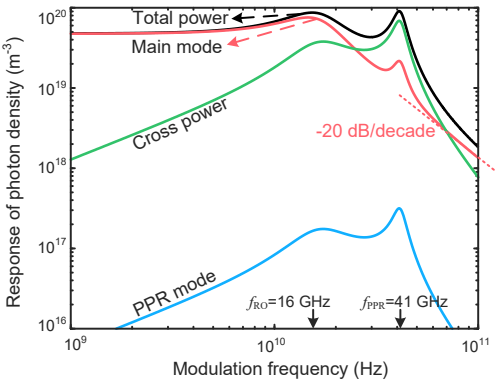

Fig. 4 Small signal response of the total power ($\delta S_a/\delta I_a$), the main mode power ($\delta S_1/\delta I_a$), the PPR mode power ($\delta S_2/\delta I_a$), the cross power ($\delta S_X/\delta I_a$), and $\delta S_a = \delta S_1 + \delta S_2 + \delta S_X$. f_{RO}: the relaxation oscillation frequency, f_{PPR}: the PPR frequency. $\Delta\lambda_6$ = 0.446 nm.

The response of the main mode power $\delta S_1/\delta I_a$ (red line) is strongest at the relaxation oscillation frequency. The decay rate of $\delta S_1/\delta I_a$ at high frequencies is -20 dB/decade, which is the same as the decay rate of the AM response of a laser diode without PPR effect (Coldren 2012). The response of the PPR mode power $\delta S_2/\delta I_a$ (blue line) is also much smaller and seems can be neglected.

In Fig. 4, notability, the response of the cross power $\delta S_X/\delta I_a$ (green line) is strongest at the PPR frequency and so it is manifested as the main contribution to the PPR peak. This can be understood by comparing (14) and (15), the difference between them is that for the response of the cross power, the MTF $\delta f_2/\delta I_a$ is multiplied by the complex amplitude of the main mode f_{1s}, which means that the main mode amplifies the response of the PPR mode and initiates the PPR effect. This demonstrates that the PPR mode "is not lasing and acts as a catalyst" (Morthier 2000). Moreover, the response of the cross power has a decay rate faster than -20 dB/decade at high frequencies, which results in a sharper PPR peak than the relaxation oscillation peak.

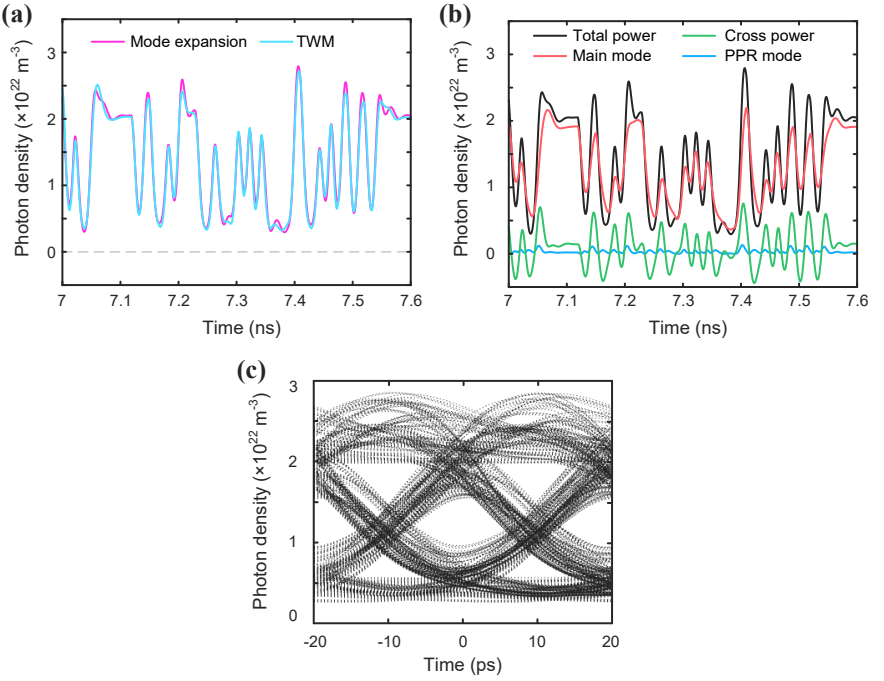

Fig. 5a Time domain waveforms calculated by the model expansion rate equations (purple line) and TWM (cyan line) under large signal modulation at 50 Gb/s. **b** Time domain waveforms of total power S_a (black line), main mode power S_1 (red line), PPR mode power S_2 (blue line), and cross power S_X (green line) under the same modulation signal as in **a**. **c** Eye Diagram at 50 Gb/s. $\Delta\lambda_6 = 0.446$ nm.

Finally, large-signal dynamics of the DBR laser when PPR occurs is discussed. Time domain waveforms of 50 Gb/s nonreturn-to-zero (NRZ) pseudo-random bit sequence (PRBS) large signal modulation are shown in Fig. 5a, calculated by the mode expansion rate equations (3)-(5) and TWM. It can be seen that the waveforms of the total optical power calculated by the mode expansion method and TWM are well matched.

In addition, the total optical power in the DBR laser can be decomposed into three components using the mode expansion method, as shown in Fig. 5b. The main mode power S_1 (red line) is the main part of the total power, whose eye diagram should be closed at such a high modulation rate. The PPR mode power S_2 (blue line) is much lower than the other two powers and can be ignored. The amplitude of the cross power S_X (green line) is large

when “0 bit” and “1 bit” alternate, while it is small with successive "0 bit" or "1 bit", confirming that the cross power is band-passed at the PPR frequency. The cross power can be negative, representing the energy exchange between the main mode and the PPR mode. Constructive interference between the cross power and the main mode power enhances the responsibility at high modulation rates, indicating that the cross power is the main contributor to the PPR effect. The eye diagram of 50 Gb/s modulation is shown in Fig. 5c. With the help of the PPR effect, the eye diagram of the DBR laser is open.

5 Conclusion

The mode dynamics behind the PPR effect of DBR lasers is clarified by solving the mode expansion rate equations. The PPR effect is related to the coupling factors in the rate equations, as well as the cross-power term in the photon density, both of them are determined by the overlap integrals of the mode patterns in the cavity. Analysis of the small signal modulation response indicate that the cross power is the main contributor to the PPR peak, and the enhancement of the PPR peak is clearly observed with a decrease in the threshold gain difference and with an increase in the coupling factors and cross power. Simulations of large signal dynamics demonstrate that the cross power can help the eye diagram to open up at high baud rates. Compared with the pure TWM, the mode expansion rate equations are helpful to understand the mode interaction processes during the PPR effect.

Acknowledgements This work was supported in part by the National Natural Science Foundation of China (No. 61675073), and in part by Wuhan International Joint Laboratory on Optoelectronics.

Reference

Matsui, Y., Schatz, R., Pham, T., Ling, W. A., Carey, G., Daghighian, H. M., Adams D.: 55 GHz bandwidth distributed reflector laser. Journal of lightwave technology, 35(3), 397-403 (2017)

Kjebon, O., Schatz, R., Lourdudoss, S., Nilsson, S., Stalnacke, B., Backbom, L.: 30 GHz direct modulation bandwidth in detuned loaded InGaAsP DBR lasers at 1.55μm wavelength. Electronics Letters, 33(6), 488-489 (1997)

He, J. J.: Proposal for *Q*-Modulated Semiconductor Laser. IEEE Photonics Technology Letters, 19(5), 285-287 (2007)

Morthier, G., Schatz, R., Kjebon, O.: Extended modulation bandwidth of DBR and external cavity lasers by utilizing a cavity resonance for equalization. IEEE Journal of Quantum Electronics, 36(12), 1468-1475 (2000)

Mieda, S., Yokota, N., Kobayashi, W., Yasaka, H.: Ultra-wide-bandwidth optically controlled DFB laser with external cavity. IEEE Journal of Quantum Electronics, 52(6), 1-7 (2016)

Matsui, Y., Schatz, R., Che, D., Khan, F., Kwakernaak, M., Sudo, T.: Low-chirp isolator-free 65-GHz-bandwidth directly modulated lasers. Nature Photonics, 15(1), 59-63 (2021)

Tager, A. A., Elenkrig, B. B.: Stability regimes and high-frequency modulation of laser diodes with short external cavity. IEEE journal of quantum electronics, 29(12), 2886-2890 (1993)

Bardella, P., Montrosset, I.: A new design procedure for DBR lasers exploiting the photon–photon resonance to achieve extended modulation bandwidth. IEEE Journal of Selected Topics in Quantum Electronics, 19(4), 1502408-1502408 (2013)

Radziunas, M., Glitzky, A., Bandelow, U., Wolfrum, M., Troppenz, U., Kreissl, J., Rehbein, W.: Improving the modulation bandwidth in semiconductor lasers by passive feedback. IEEE Journal of selected topics in Quantum Electronics, 13(1), 136-142 (2007)

Radziunas, M., Wünsche, H. J.: Multisection lasers: longitudinal modes and their dynamics. In Optoelectronic devices (pp. 121-150). Springer, New York (2005)

Feiste, U.: Optimization of modulation bandwidth in DBR lasers with detuned Bragg reflectors. IEEE journal of quantum electronics, 34(12), 2371-2379 (1998)

Huang, W. P.: Coupled-mode theory for optical waveguides: an overview. JOSA A, 11(3), 963-983 (1994)

Coldren, L. A., Corzine, S. W., Mashanovitch, M. L.: Diode lasers and photonic integrated circuits (Vol. 218). John Wiley & Sons (2012)

Chaciński, M., Schatz, R.: Impact of losses in the Bragg section on the dynamics of detuned loaded DBR lasers. IEEE journal of quantum electronics, 46(9), 1360-1367 (2010)